A Geochemical and Geophysical Characterization of Sulfide Mine Ponds at the Iberian Pyrite Belt (Spain)

Tomás Martín-Crespo · Silvia Martín-Velázquez ·
David Gómez-Ortiz ·
Cristina De Ignacio-San José · Javier Lillo-Ramos

Abstract This work presents the results of a geochemical and geophysical characterization of the Monte Romero and La Naya mine ponds, belonging to the Cueva de la Mora and Riotinto mine districts, respectively, based on mineralogical, geochemical and geophysical techniques. In order to obtain a representative environmental characterization, two deposits showing different mineralogies, physico-chemical parameters, chemical compositions of tailings and pond conditions were selected. Monte Romero mine tailings showed an upper level mainly composed of silicates and a deeper level mainly composed of sulfides and barite. The toxic metal content was different in both levels but high enough to exceed the regional legal concentration limits for agricultural soils. An electrical resistivity tomography survey revealed a homogeneous upper unit (3 m thickness), which displayed low resistivity values, corresponding to water-saturated silt and clay materials with an abundance of sulfides which was interpreted as the pond infilling. The La Naya mine pond presented a homogeneous mineralogical composition made up of quartz as the main mineral and chlorite-smectite and jarosite as accessory phases. The absence of sulfide phases and the low contents of metal elements are directly related to the reworking processes of the sludge dumped in this pond. The geophysical survey revealed that the pond infilling did not have a constant thickness, but ranged between 15 and 20 m. An inner groundwater flow in the infilling was recognized. The low resistivity values allowed the presence of acid waters and related subsurface flows to be identified in both mine ponds, but no acid water drainage occurred across their vessels. When compared to the Aznalcóllar tailings spill, the La Naya pond is large enough to release a similar amount of sludge, but of a very low metal content. The Monte Romero sludge displays a similar, potentially toxic metal content to the Aznalcóllar sludge, but its size is significantly smaller.

T. Martín-Crespo (✉) · S. Martín-Velázquez ·
D. Gómez-Ortiz · J. Lillo-Ramos
Dpt. Biología y Geología, ESCET,
Universidad Rey Juan Carlos,
C/Tulipán s/n,
28933 Móstoles, Madrid, Spain
e-mail: tomas.martin@urjc.es

S. Martín-Velázquez
e-mail: silvia.martin@urjc.es

D. Gómez-Ortiz
e-mail: david.gomez@urjc.es

J. Lillo-Ramos
e-mail: javier.lillo@urjc.es

C. De Ignacio-San José
Dpt. Petrología y Geoquímica, Fac. CC. Geológicas,
Universidad Complutense de Madrid,
C/Antonio Novais s/n,
28040 Madrid, Spain
e-mail: cris@geo.ucm.es

1 Introduction

The volcano-sedimentary rocks of the Iberian Pyrite Belt, in the southwest (SW) of the Iberian Peninsula, host one of the largest concentrations of massive sulfide mineralizations in the world, which were formed during the Variscan Orogeny (e.g. Leistel et al. 1998; Sáez et al. 1996; Tornos 2006; and references therein). Pyrite is the main metallic mineral, although sphalerite, galena, chalcopyrite and arsenopyrite are also found in lower quantities. An intense mining activity in this province, which goes back to the Third millennium B. C. (van Geen et al. 1997; Nocete et al. 2005; Ruiz et al. 1998), is related to the exploitation of S-Cu–Pb–Zn from the sulfide ore bodies and, to a lesser extent, to Ag–Au (Fig. 1).

Owing to the extraction and metallurgic processes, a huge amount of mine installations, galleries and waste deposits has been generated in SW Iberia, and they are a continuing source of severe environmental contamination. Pollution from these sources can be originated via mining spills, leakages or wind-blown dust, and toxic elements with a high mobility can cause huge environmental problems by accumulating in flora and fauna and reducing the quality of streams and groundwater (Siegel 2002). Several studies have highlighted the elevated concentrations of certain trace elements in sediments and soils surrounding mining or waste sites in the Iberian Pyrite Belt as a consequence of extraction and metallurgic processes (Chopin and Alloway 2007; Fernández-Caliani et al. 2009; Galán et al. 2002; López et al. 2008). This mine-related contamination also reaches the waters of the Tinto and Odiel fluvial systems, with low pH values and large volumes of sulfates, metals and metalloids (Cánovas et al. 2007, 2008; Fernández-Remolar et al. 2005; Hudson-Edwards et al. 1999; Sánchez España et al. 2005, 2008; Sarmiento et al. 2009). Finally, a significant amount of metal is transferred to the sediments of the Tinto-Odiel estuary (van Geen et al. 1997; Ruiz et al. 1998).

A great amount of fine waste material from mining activities is specifically disposed of in a slurry form in tailings dams, i.e., structures designed to settle and store tailings and process water (Vick 1990). These watery sludges are composed of medium-to-fine-grained particles (0.01–1.5 mm) resulting from grinding and mineral processing. Although the metal content is removed in the metallurgic process, some ores and sulfides (e.g., pyrite, chalcopyrite and arsenopyrite) can be deposited, either because they were not sufficiently for use, or due to a deficient extraction technology. Oxidation of the sulfide grains accumulated in the abandoned mine tailings may take place which results in (1) acid leakages and highly contaminating acid mine drainage (AMD) and (2) the mobilization of significant quantities of trace elements such as As, Cd, Cu, Hg, and Pb (Cánovas et al. 2007; Siegel 2002). Because of this, it is necessary to identify and characterize these hazardous areas where large quantities of potentially toxic elements can be released into the environment.

The mining industry in the province of Huelva left 19 tailings dumps; 11 are in an abandoned state (IGME 1998) and represent an important contamination problem (Acero et al. 2007; Álvarez-Valero et al. 2009; Hudson-Edwards et al. 1999; Pérez-López et al. 2007; Sánchez España et al. 2005). Remediation has only been carried out in a few of the dumps, although they still show significant environmental problems (Martín-Crespo et al. 2010). In fact, an environmental disaster occurred in the SW of Spain in 1998, when the tailings dam of the Los Frailes Pb–Zn mine at Aznalcóllar (Seville; Fig. 1) was ruptured, and $\sim 2 \times 10^6$ m^3 of heavy metal-bearing sludge and $\sim 4 \times 10^6$ m^3 of acidic waters were released (Aguilar et al. 2004, 2007; Galán et al. 2002; Hudson-Edwards et al. 2003).

In order to obtain a representative characterization of mine ponds as a result of the extensive mining activity at the Riotinto district (the Iberian Pyrite Belt), two different ore deposits were selected: the Monte Romero and La Naya mine ponds (Fig. 1). Different mineralogies, physico-chemical parameters, chemical compositions of tailings and different pond conditions (size, geometry, structure, thickness, water flows, and visual integration with the environment, amongst others) have been described. Monte Romero comprises two small contiguous mine ponds located at the Cueva de la Mora mine site, where Pb- and Zn-bearing minerals were mined and processed (IGME 1998). La Naya is a mine pond located 2.5 km to the southeast of Minas de Riotinto town, in the heart of the Iberian Pyrite Belt, and is one of the largest deposits generated during the extensive mine works in the Riotinto mining group. Pyrite and Cu-bearing minerals were the main minerals extracted (IGME 1998).

In this work, we applied mineralogical and geochemical characterization techniques (X-ray diffraction,
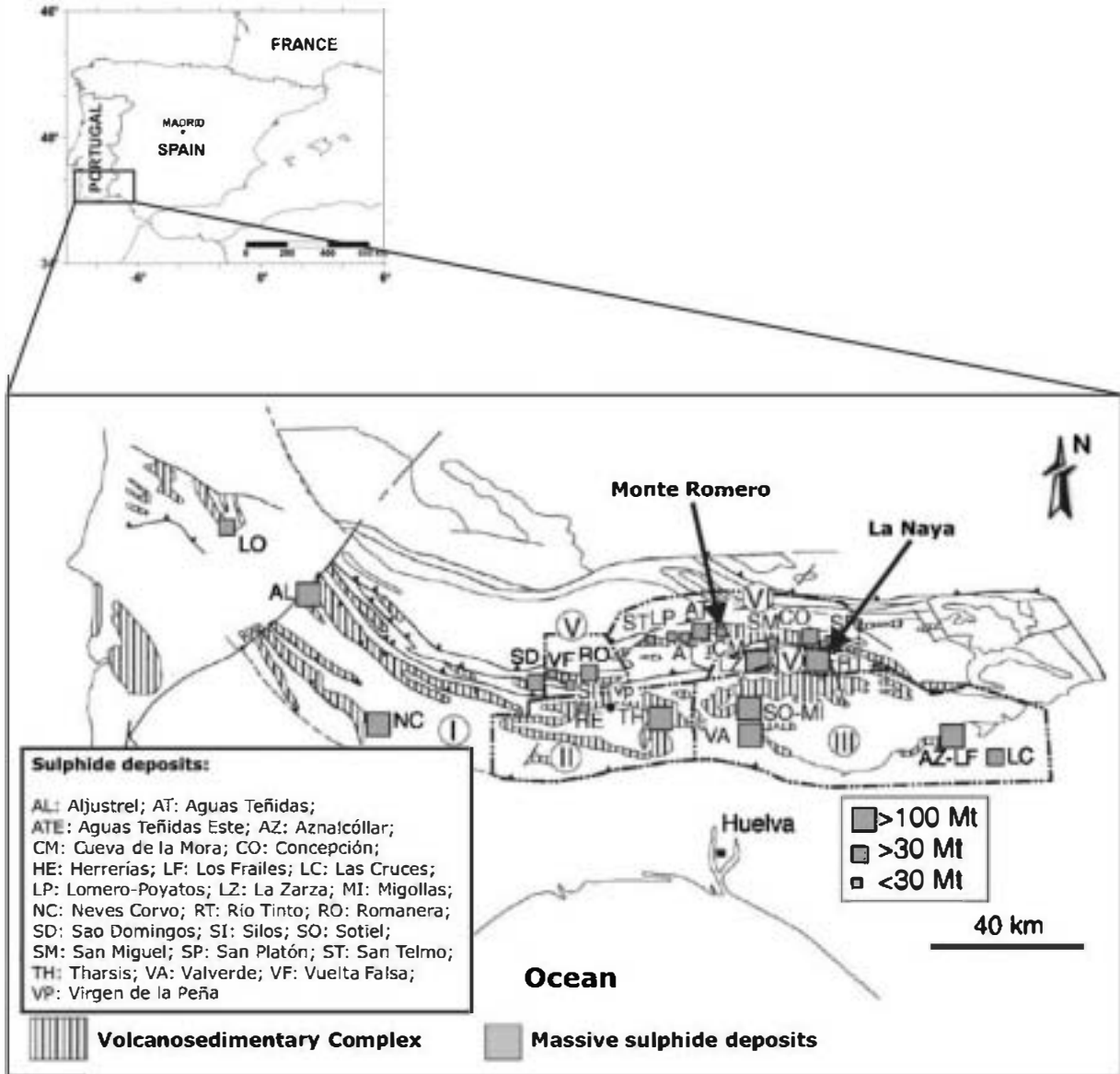
Fig. 1 Location of the Monte Romero and La Naya mine ponds, the different metalogenic domains and the main massive sulfide deposits of the Iberian Pyrite Belt. Modified from Tornos (2006). Metalogenic domains: *I* Western Domain, *II* Puebla de Guzmán Domain, *III* Sotiel-Aznalcóllar Domain, *IV* Rio Tinto Domain, *V* Paymogo Domain, *VI* Northern Domain

environmental scanning electron microscopy (ESEM) coupled with energy dispersive X-ray analysis (EDX), X-ray fluorescence, instrumental neutron activation analysis (INAA) and inductively coupled plasma mass spectroscopy-ICP-MS) and a shallow, non-destructive geophysical technique (electrical resistivity tomography) to obtain a detailed picture of the mine pond geometry, composition and thickness of infilling, the possible existence of water flows within and the occurrence of acid mine drainage leakages. The pH parameter was also measured to determine the acidic conditions of the impoundments. Thus, the main objective was to characterize the present conditions of the ponds to identify any related environmental problems. The goal of this research was particularly relevant because although the mining activity in this region has decreased over the past few decades, mine wastes remain a continuing source of AMD and metal contamination, and soils and watercourses in southwest Iberia are still highly polluted.

2 Location and Features of the Mine Ponds

The Monte Romero mine ponds, nowadays abandoned, are located near the Cueva de la Mora village (Fig. 2a, b). Both are quite similar and were produced as a result of metallurgic extraction of sphalerite and galena by the company Asturiana de Zinc S.A. (IGME 1998). Their gray tailings lie over Carboniferous shales, which represents the main outcropping lithology in the area. The layout of this storage installation had a side-hill impoundment design with an upstream method of construction (IGME 1998). The dimensions of the ponds are 125×80 m for the westernmost one and 90×70 m for the easternmost one, both of which are divided by a small topographic escarpment. During the field survey, both mine ponds become flooded in the northernmost parts and the water table in the western pond was located at a maximum depth of 0.5 m, as would be observed in a small ditch. For these ponds, Blanco et al. (2003) described water table depths ranging from 0.5 m during winter to about 3 m during summer. Moreover, water flows towards the tailing surfaces were described in shallower levels (50 cm depth) after intense rainfall-evaporation episodes by Blanco et al. (2003). In this case, water drains from the ponds into a small local creek (Monte Romero creek) by means of a plastic pipe.

The La Naya mine pond (Fig. 2c e), with an extension of 500×300 m, was formed as a result of the exploitation of an old mine belonging to the Riotinto mining district, mainly for pyrite, copper and gold, by the company Riotinto Minera S.A. (IGME
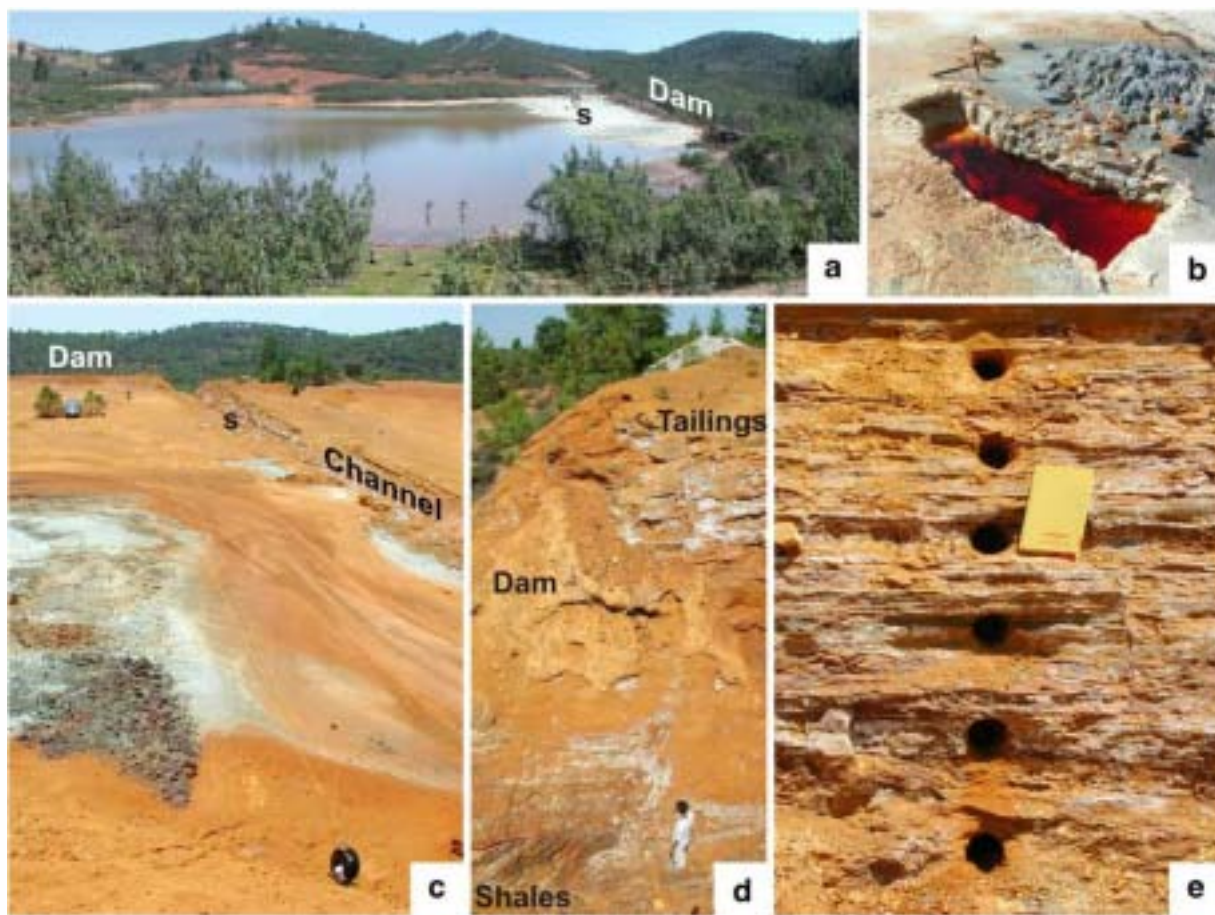

Fig. 2 a General view of the western Monte Romero mine pond. The tailings sampling(s) was done in a previous survey with a lower level of the ponded water, b a ditch in the mine sludges of Monte Romero shows the shallow water table in the tailings and the acid nature of the water, denoted by the characteristic red color; c general view of the La Naya mine pond and its long discharge channel, where the tailings sampling (s) was performed; d La Naya dam and impoundment deposited over the Devonian shales; e detail of the sampling in the laminated tailings of the channel wall in the la Naya mine pond

1998). Its northernmost part lies directly over Carboniferous basic lava flows and tuffs, whereas the southern part of the pond is located over a succession of Devonian shales, greywackes, and quartzites. A significant feature of these tailings is the marked contrast between their yellow to light brown color and the dark green color of the surrounding environment. A raised embankment was constructed using an upstream method with a valley dam configuration (IGME 1998). This deposit is one of the largest ponds in the Riotinto district, and visual integration with the environment has not been achieved. The pond includes drainage systems to control the phreatic surface and to minimize the chance of a build-up of pore-water pressures. Thus, chimney drains were installed within the slurry impoundment. This kind of structure is well suited to conditions where large volumes of water may be stored along with solid tailings (Vick 1990). Regardless of these drainage systems, the tailings dam shows a marked evidence of rain water erosion.

3 Methodology

3.1 Sampling Description

Samples from the mine tailings were collected with an Eijkelkamp soil core manual sampler for undisturbed samples with a known volume and diameter, at a sampling depth of 2 m in Monte Romero western pond and 2.7 m in the La Naya pond (Fig. 2a, c). Sampling was sequential with a vertical constant spacing of 10 cm, except for the deepest samples from the Monte Romero pond with an increased spacing. In the Monte Romero mine pond, sampling was carried out by digging down below the pond surface, casting aside the parts corresponding to superficial sealing and avoiding falling perforation wall material. Using this procedure, 15 samples were collected between 10 and 200 cm depth. In the La Naya mine pond, sampling was carried out at different depths at the wall of a discharge channel between 190 and 270 cm and nine samples were collected (Fig. 2e). The climate of both mine sites is continental Mediterranean; the average temperature is 18°C, with mild winters and hot summers denoting a seasonal variability. The sampling was conducted in June.

3.2 Mineralogical and Geochemical Methods

The techniques applied in the present study were the usual ones used for these kinds of residues. Mineralogical characterization of the mine tailings was performed by X-ray diffraction (XRD), using a Philips X'Pert powder device with a Cu anticathode and standard conditions: speed 2° 2θ/min between 2° and 70° at 40 mA and 45 KV. The study of the total sample was made by crystalline powder diffraction (non-oriented powder) on a side-loading sample holder. Semi-quantitative results were obtained by the normalized reference intensity ratio method. The mineralogy of the samples was also studied by ESEM, coupled with EDX, using a Philips XL30 microscope. The ESEM was operated at a low-vacuum mode, at a pressure of between 0.5 and 0.6 Torr under a water vapor atmosphere and an operating voltage of 20 kV. The XRD and ESEM-EDX analyses were performed at the Centro de Apoyo Tecnológico (CAT Universidad Rey Juan Carlos, Móstoles, Spain, http://www.urjc.es/cat). The Fe_2O_{3total} and trace elements were analyzed by INAA at Activation Laboratories Ltd. (1428 Sandhill Drive, Ancaster, Ontario, Canada, http://www.actlabs.com). Copper and Pb were analyzed by X-ray fluorescence with a SHIMADZU EDX-900HS analyzer at the Escuela Universitaria Politécnica de Almadén (Ciudad Real, Spain). The certified reference standard used was NIST2711.

In total, 37 minor trace elements were analyzed, although only 12 were chosen for this study (Ag, As, Au, Ba, Co, Cr, Cu, Hg, Pb, Sb, Sc, and Zn) owing to their abundance in these types of sludges and also because most of them are included in the priority contaminant list of the Andalusian regional government (Aguilar et al. 1999) and environmental protection agencies (US EPA 1993).

3.3 pH Determination

The pH of the tailings was measured in each sample from both mine ponds using an electronic pH-meter (CRISON) which was calibrated at two points (pH 7 and pH 4) using standard buffer solutions. This parameter was determined in a slurry system with an air-dried sample (10 g) mixed with distilled water (25 mL). Before reading the pH values, these solutions were vigorously stirred in a mechanical shaker for 10 min and left to stand for 30 min.

3.4 Geophysical Methods

Electrical resistivity tomography (ERT) is a geophysical prospecting technique designed for the investigation of areas with a complex geology. This technique is usually carried out using a large number of electrodes, 24 or more, connected to a multi-core cable. A laptop microcomputer with an electronic switching unit is used to automatically select the four relevant electrodes for each measurement (Loke 2004). Since an increasing separation between the electrodes provides information from increasing depths, the apparent resistivity measured can be inverted to provide a cross-section of the true resistivity along the survey line (Reynolds 1997; Telford et al. 1990). Several standard electrode arrays are available with different horizontal and vertical resolutions, penetration depths and signal-to-noise ratios (e.g. Sasaki 1992). Among them, the most frequent are the dipole–dipole, Wenner, and Wenner–Schlumberger arrays. In order to combine a good penetration depth, a reasonable vertical and horizontal resolution and a good signal-to-noise ratio, the Wenner–Schlumberger array was chosen for this study. This array was successfully used in similar studies (e.g., Martín-Crespo et al. 2010; Martínez-Pagán et al. 2009).

A Syscal Junior Switch 48 was used in this work. Three ERT profiles were performed to obtain a full characterization of the mine ponds. Their lengths range from 87.25 to 235 m and electrodes were spaced at distances of 1.75 and 5 m apart, respectively, to obtain an approximate maximum penetration depth of 25 m (Bernard 2003). The field data included resistance measurements between the various electrodes and related geometrical information. An apparent resistivity value was calculated using the resistance measurements and the geometry of the array. These data were plotted as a pseudo-section, which is a plot of the distribution of the apparent resistivity values based on the geometry of the electrodes. Pseudosections are inconclusive; therefore, they need to be inverted into sections of true resistivity values and depths via a data inversion procedure which facilitates interpretation. In this study, the inversion of resistivity data was performed using the RES2DINV code (Loke and Barker 1995, 1996).

4 Results and Discussion

The results of the mineralogical and geochemical characterization of the sampled mine tailings and of the geophysical study concerning the geometry and structure of the pond and the possible presence of acid water flows circulating from the surface to depths are presented here.

4.1 Mineralogical Characterization

The semi-quantitative data on the mineralogical composition of the Monte Romero and La Naya mine ponds are displayed in Table 1.

4.1.1 Monte Romero Mine Ponds

Two levels showing different and homogeneous mineralogical compositions can be inferred from the X-ray diffraction data (Table 1): (1) an upper level mainly composed of silicates as the dominant phase and (2) a deeper level mainly composed of sulfides and sulfates as the dominant phases. Samples from the first level (1), from the surface to 70 cm in depth, were mainly composed of quartz, illite, feldspar, and chlorite as the main minerals, with jarosite, pyrite, gypsum, copiapite, and galena in minor quantities. The scheme of Jambor and Owens (1993) was used for tailing-mineral identification: primary minerals or those minerals that constitute ore and gangue assemblages and which were originally deposited in the waste dumps; and secondary minerals, which were deposited within the dumps by precipitation from metal-rich waters derived from AMD. From the semi-quantitative analyses it could be observed that silicate minerals made up 70–90 wt.% of the total minerals, from which quartz made up 55 wt.%. Pyrite and gypsum were only identified in the deepest samples of this shallower zone (50–70 cm depth), which yielded the lowest quartz content. Jarosite, a hydrated K–Fe sulfate ($KFe^{3+}(SO_4)_2 \cdot (OH)_6$), was identified in all of the studied samples from 10 to 70 cm depth, although the highest contents were associated with non-sulfide samples (10-40 cm depth). Copiapite, a hydrated Fe sulfate ($Fe^{2+}Fe_4^{3+}(SO_4)_6(OH)_2 \cdot 20(H_2O)$), was been identified in samples collected at 40–50 cm depth as an accessory mineral. The presence of jarosite and copiapite in this first level could be related to Fe-sulfide oxidation and water flows. Primary sulfide minerals (e.g., galena) identified in low amounts by X-ray diffraction were also

Table 1 Semi-quantitative mineralogical composition (wt.%) of the studied samples from the mine tailings

Zone	Sample	Depth (cm)	Qtz	Fsp	Ill	Chl	Ja	Gp	Co	Ga	Py	Sp	Ba	Gt
Monte Romero	R-10	10	50	10	20	5	10	–	–	5	–	–	–	–
	R-20	20	55	10	15	5	10	–	–	5	–	–	–	–
	M-30	30	55	10	15	5	10	–	–	5	–	–	–	–
	M-40	40	50	15	15	5	10	–	5	–	–	–	–	–
	M-50	50	40	10	25	10	5	5	5	–	10	–	–	–
	M-60	60	35	10	20	5	5	5	–	–	10	–	–	–
	M-70	70	35	15	20	5	5	10	–	–	10	–	–	–
	M-80	80	20	5	–	–	–	–	–	–	45	10	20	–
	M-90	90	25	5	–	–	–	–	–	–	45	10	15	–
	M-100	100	25	5	–	–	–	–	–	–	35	10	25	–
	M-110	110	25	5	–	–	–	–	–	–	35	15	20	–
	M-120	120	20	10	–	–	–	–	–	–	40	15	15	–
	M-140	140	20	10	–	–	–	–	–	–	45	10	15	–
	M-150	150	25	5	–	–	–	–	–	–	40	15	15	–
	M-200	200	25	10	–	–	–	–	–	–	40	10	15	–
La Naya	N-190	190	85	–	–	10	5	–	–	–	–	–	–	–
	N-200	200	85	–	–	10	5	–	–	–	–	–	–	–
	N-210	210	80	–	–	10	5	–	–	–	–	–	–	5
	N-220	220	75	–	–	10	5	5	–	–	–	–	–	–
	N-230	230	85	–	–	10	5	–	–	–	–	–	–	–
	N-240	240	90	–	–	5	5	–	–	–	–	–	–	–
	N-250	250	70	–	–	10	5	–	–	–	10	5	–	–
	N-260	260	85	–	–	5	5	–	–	–	–	–	–	5
	N-270	270	85	–	–	5	5	–	–	–	–	–	–	5

Qtz quartz, *Fsp* feldspar, *Ill* illite, *Chl* chlorite, *Ja* jarosite, *Gp* gypsum, *Co* copiapite, *Ga* galena, *Py* pyrite, *Sp* sphalerite, *Ba* barite, *Gt* goethite

recognized in this upper level as minor species by ESEM-EDX. Galena occurred as idiomorphic isolated cubic crystals commonly showing octahedron exfoliated faces. Secondary electron images revealed that pyrite crystals frequently occurred intergrowing with other primary gangue minerals such as quartz and chlorite-smectites or hydrated Fe sulfates. Barite and sphalerite were not recognized by either ESEM-EDX or XRD.

The deeper level (2) was mainly composed of sulfides (pyrite and sphalerite) and sulfates (barite) and comprises samples from 80 to 200 cm depth (M80 to M-200). The pyrite content ranged between 35 and 45 wt.%, sphalerite between 10 and 15 wt.% and barite between 15 and 25 wt.%. At this level, only a 30 wt.% of silicate minerals (quartz and feldspar) were determined. The primary gangue, host rock minerals and secondary minerals were identified from the ESEM-EDX studies. Idiomorphic crystals of barite, galena and pyrite frequently occurred as aggregates, as part of the ore paragenesis.

The Monte Romero mine pond still preserves a relatively high proportion of primary (original ore) mineral phases, such as abundant pyrite with subordinate sphalerite and traces of galena, accompanied by gangue minerals. The mineralogical composition determined (Table 1) is similar to that previously reported by Acero et al. (2007) for 50 cm depth sludge from this mine pond. The distribution of phases was clearly arranged in two different levels; the shallower level concentrated secondary minerals, mainly represented by hydrated iron sulfates (jarosite, copiapite) and gypsum, whereas the deepest level retained abundant sulfides and barite. It is noteworthy that at the depth of 70 cm the boundary between these two zones was very sharp with a complete downwards disappearance of some gangue minerals, such as illite and chlorite, whereas others exhibited an abrupt increase, as was the case for barite. This may indicate two different provenances for each of the distinguished levels.

4.1.2 La Naya Mine Pond

A homogeneous mineralogical composition made up of quartz as the main mineral, and chlorite-smectite and jarosite as accessory mineral phases, was defined in the X-ray diffraction study in all samples from La Naya (Table 1). Goethite was only identified as an accessory mineral phase in three samples (N-210, N-260, and N-270). Quartz made up 90 wt.% of the total minerals. Gypsum was only identified in one sample (N-220). Other silicate phases such as illite or feldspar were not identified. Although sulfide phases are typically present in this type of mine tailings, only pyrite and sphalerite were identified in significant amounts (10 and 5 wt.%, respectively) in one sample (N-250, 250 cm depth). It is important to highlight that jarosite was identified in all of the studied samples. Other sulfide phases such as arsenopyrite, chalcopyrite and galena were not detected by X-ray diffraction. The main secondary mineral phases recognized by ESEM-EDX were Fe-oxyhydroxides. Ochreous to brown cryptocrystalline Fe-oxyhydroxides commonly occurred around other mineral phases such as quartz, and completely or partially replaced primary sulfide grains such as pyrite and sphalerite. Pyrite was the main sulfide mineral in the tailings, occurring as submillimetric idiomorphic cubic crystals, some of which were pseudo-morphologically replaced by aggregates of Fe-oxyhydroxides. Flake-shaped Fe-rich chlorite-smectite crystals were detected in minor quantities in the alteration rims of sulfide grains, together with Fe-oxyhydroxides.

The La Naya mine pond composition was strongly dominated by quartz with very low contents of primary sulfides and even secondary minerals. Such a "residual" composition probably indicates that reworking of the slag-heaps and their processing with enhanced metallurgic techniques had taken place, leaving a much more sterile and thus less hazardous situation from the environmental point of view than in Monte Romero.

4.2 Geochemical Constraints

The chemistry analyses also confirmed that the two sites studied were very different in terms of their major and trace element concentrations. The Fe_2O_3 $_{total}$, trace element concentrations and pH measurements at the different sampling depths from Monte Romero and La Naya mine ponds are shown in Table 2. In addition to this, the tailings samples show an important acidity with a pH interval from 2.5 to 3.5. The most acidic values corresponded to the Monte Romero mine pond, with the lowest at 50 cm depth (pH=2.5) and a mean pH level of pH 2.9. The La Naya deposit had a mean pH level of pH 3.2, although an increasing trend with depth was found.

4.2.1 Monte Romero Mine Ponds

The composition of the Monte Romero mine sludge was characterized by high contents of Ba, As, Fe and other heavy and transitional metals. Such a high Ba content was related to the ore mineral assemblage, where barite was one of the paragenetic phases. The Fe_2O_3 $_{total}$ content ranged between 2.1 and 27.2 wt.%, Cu between 914 and 16,582 ppm, Pb between 295 and 12,610 ppm and the Zn content was up to 41,800 ppm. Other trace elements which displayed high values were: Au (up to 720 ppm), As (up to 2,740 ppm) and Sb (up to 861 ppm). These are important amounts in all cases, although unsurprisingly due to the type of mineralization that was exploited, which was fundamentally composed of pyrite (FeS_2), chalcopyrite ($CuFeS_2$), sphalerite (ZnS) and galena (PbS), with arsenopyrite ($FeAsS$), magnetite (Fe_3O_4) and tetrahedrite-group minerals in minor amounts (Tornos 2006). Galena appeared to be associated with the minor gold values found in the ores. The Hg content was related to the formation of a replacive mineralization, the precipitation of an epithermal trace element suite (Au, As, Sb, and Hg), barite-rich zones and a high sulfidation mineral assemblage (Tornos 2006). The Ni content was below the detection limit (20 ppm) in each of the analyzed samples. Significant variations as a function of depth were identified in all of the analyzed element contents (Table 2; Fig. 3). This variation defined a pattern with the two depth intervals showing different metal contents. These depth intervals are separated with a dotted line at 70 cm depth in Fig. 3. This pattern correlated with the mineralogy in that the lowest metal contents occurred between 10 and 70 cm depth, whereas the highest contents were located between 80 and 200 cm depth. Mercury, Pb, Sb, and Sc displayed an inverse concentration pattern compared to the rest of the elements, with their lowest concentrations occurring in the deeper interval. Within the shallower depth interval, the preferential concentration of copper at the 60–70 cm depth was

Zone	Sample	Depth (cm)	Ag (ppm)	As (ppm)	Au (ppb)	Ba (ppm)	Co (ppm)	Cr (ppm)	Cu (ppm)	Fe_2O_3 total (wt.%)	Hg (ppm)	Pb (ppm)	Sb (ppm)	Sc (ppm)	Zn (ppm)	pH
Monte Romero	R-10	10	70	1190	412	7740	b.d.	b.d.	1799	4.31	25	12610	502	6.8	1200	2.97
	R-20	20	55	1110	450	6840	b.d.	b.d.	914	2.12	30	10602	449	6.8	520	3.05
	M-30	30	50	1320	365	7560	b.d.	b.d.	2320	2.81	26	11658	487	6.7	710	2.95
	M-40	40	42	2740	311	7020	2	b.d.	2880	4.34	21	9876	432	8	1410	2.56
	M-50	50	37	2530	299	11700	2	24	1944	4.73	18	7739	318	6.9	2120	2.51
	M-60	60	81	2320	596	20700	8	b.d.	15278	9.81	45	6835	861	5	7970	2.79
	M-70	70	59	1580	665	23400	7	15	16582	8.89	25	4979	395	5.2	6350	3.00
	M-80	80	43	1560	720	45900	49	b.d.	5751	26	18	675	219	0.5	16100	2.99
	M-90	90	39	1710	629	60300	39	16	3758	21.8	19	709	186	1.1	14600	3.16
	M-100	100	36	1580	662	99000	31	24	1401	19.4	11	295	186	0.6	5180	3.06
	M-110	110	45	1450	703	59400	25	b.d.	5642	18.3	34	396	211	0.8	41800	3.21
	M-120	120	53	1380	652	50400	50	21	6752	21.8	21	1136	240	0.8	20500	3.13
	M-140	140	47	1580	744	46800	55	19	3953	27.2	16	755	222	0.5	12700	3.01
	M-150	150	36	1410	613	51300	49	8	2149	24.5	11	499	190	0.8	6990	2.95
	M-200	200	31	1300	554	53100	40	b.d.	1993	22.6	10	467	168	0.8	5870	2.87
La Naya	N-190	190	b.d.	191	81	710	4	13	306	8.51	b.d.	101	31.3	2	180	2.88
	N-200	200	b.d.	347	68	990	10	5	579	9.45	b.d.	187	33.4	1.7	120	3.20
	N-210	210	b.d.	909	85	590	5	5	684	13.9	b.d.	82	50.4	2.5	210	2.84
	N-220	220	b.d.	674	77	860	16	7	772	11.2	b.d.	222	42.8	3.1	200	3.28
	N-230	230	b.d.	401	100	520	8	6	485	8.65	b.d.	163	31	1.8	120	3.51
	N-240	240	b.d.	201	49	440	3	6	583	11.2	b.d.	89	26.8	1.4	50	3.04
	N-250	250	b.d.	451	49	520	62	8	4511	12.7	b.d.	51	28.2	3.9	260	3.52
	N-260	260	b.d.	618	65	270	11	5	652	14.1	b.d.	124	37.5	1.5	70	3.13
	N-270	270	b.d.	458	55	440	3	6	412	13.9	b.d.	181	35.7	1.2	80	3.43

b.d. below detection

accompanied by the highest Sb and Ag contents. Cobalt, Ba, Fe_2O_3 total, and Zn showed a significant increase in their contents in the 80-200 cm depth interval when compared to the moderate increase of Au. Mercury and Ag, however, showed an irregular distribution with depth, displaying their maximum concentrations at 60 cm, and their second relative maxima located, respectively, at 110 and 120 cm.

Possible mining explanations for these contents and variations could be: (1) periods in which the mineral benefit was higher, either due to improvements in metallurgic processes or to the mineral being of a higher grade, which alternated with periods in which a greater proportion of the ore mineral particles were not efficiently well-exploited and ended up within these residual mine tailings; (2) a change in the exploitation targets, which originally were mainly

focused on galena (Pb) mining but were re-directed from the 1970s to pyrite (Fe) and sphalerite (Zn) mining due to environmental policies that banned the use of lead in many industrial fields; and (3) a change in the ore paragenesis between different zones within the same mine or between different mines. According to the long mining history of this mine site, the first and second options are probably the most likely ones. Moreover, the drastic decrease in pyrite concentrations, together with the occurrence of jarosite, copiapite, and gypsum in the shallow level (Table 1), attest for pyrite alterations releasing sulfate into this superficial zone. This could also have contributed to highlighting the differences.

Apart from recognizing features inherited from the respective mining histories of both mine ponds, some evolution processes in each sub-system were recognized
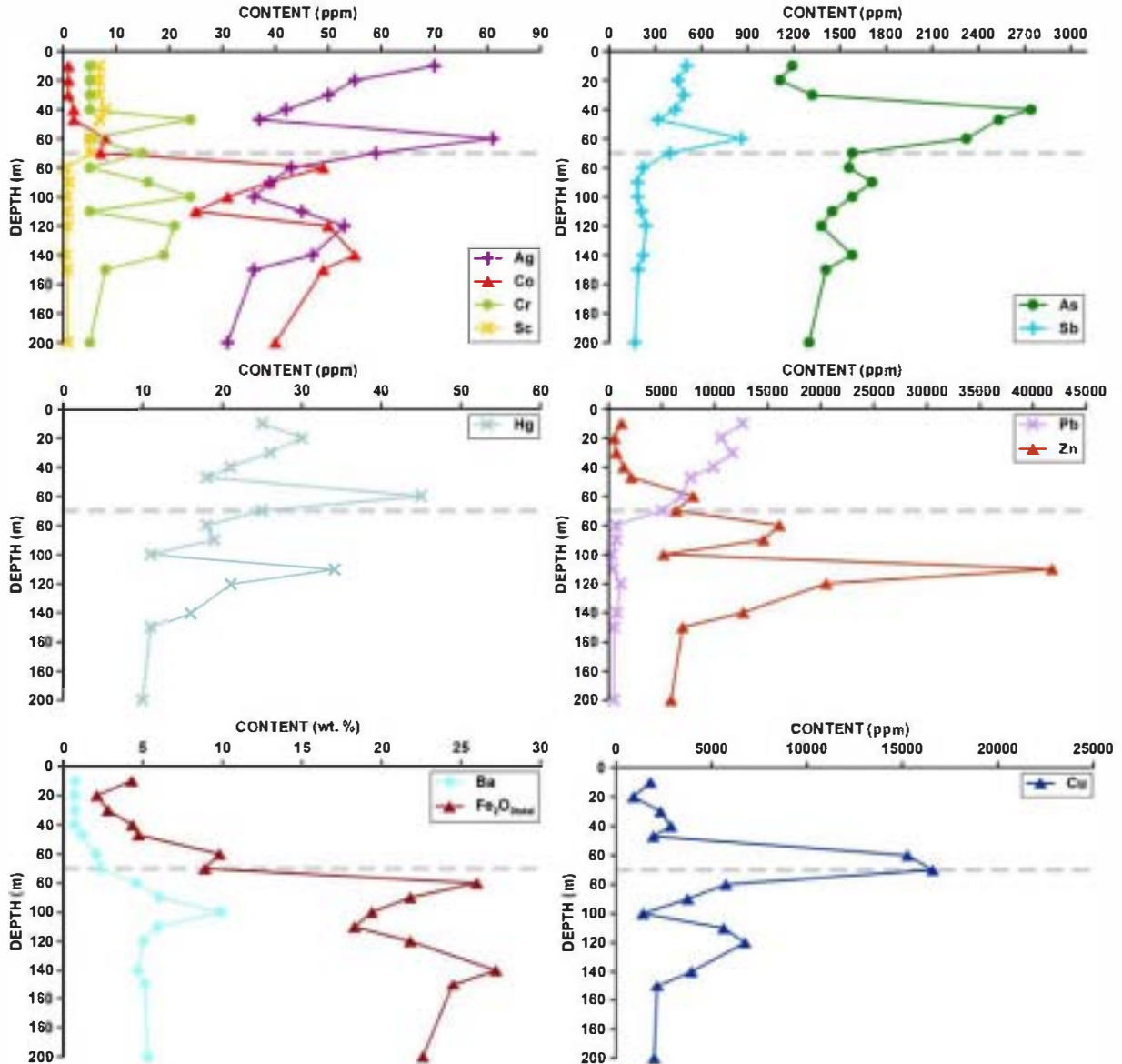
Fig. 3 Distribution-with-depth profiles for total ferric iron and trace elements concentrations from Monte Romero mine tailings

which allowed us to estimate the polluting potential of each mine. With this idea in mind, we constructed correlation matrices for both the surface (Table 3) and deep (Table 4) levels of the Monte Romero mine pond. The superficial level of the Monte Romero mine pond (10–70 cm depth) only contained pyrite as the essential sulfide phase, together with traces of galena. High, positive correlations between Fe_2O_3 total and Ba, Co, Cu, and Zn, and the absence of a correlation with Pb, indicated that Pb (galena) was not mined at this level. Elements which were not mined were concentrated at

this level of the pond and showed good correlations between them, confirming the results of previous work (Lillo et al. 2008). On the contrary, the mined elements, like Pb, showed negative correlations with the majority of the other elements. The presence of Hg in the Monte Romero ponds indicates that this element was not mined and that it became concentrated in the mine ponds. The pattern is different in the deeper zone (80–200 cm depth) of the Monte Romero mine ponds. Within this level, correlations between the elements were the same as those expected in a zone where

Table 3 Correlation matrix between elements of the shallow level (10 to 70 cm depth) of Monte Romero mine tailings (n=7; significance p<0,05)

	Ag	As	Au	Ba	Co	Cu	Fe$_2$O$_{3\ tot}$	Hg	Pb	Sb	Zn
Ag	1.00										
As	−0.31	1.00									
Au	0.70	−0.26	1.00								
Ba	0.46	0.19	0.85	1.00							
Co	0.48	0.39	0.78	0.95	1.00						
Cu	0.56	0.16	0.89	0.97	0.96	1.00					
Fe$_2$O$_{3\ tot}$	0.56	0.35	0.77	0.95	0.97	0.95	1.00				
Hg	0.83	−0.08	0.62	0.45	0.55	0.55	0.52	1.00			
Pb	−0.09	−0.44	−0.63	−0.90	−0.88	−0.82	−0.81	−0.21	1.00		
Sb	0.83	0.08	0.46	0.36	0.51	0.49	0.53	0.94	−0.10	1.00	
Zn	0.59	0.30	0.82	0.96	0.99	0.96	0.98	0.63	−0.83	0.59	1.00

sulfide mineralogy predominates. Thus, galena seemed to control both Ag and Sb (high, positive correlations, respectively; see Table 4) and, consequently, Ag and Sb showed a high correlation coefficient, which was interpreted as meaning that both elements play the same geochemical role as sulfosalts or impurities in galena. Moreover, the very high correlation coefficient (r=0.99) between Zn and Hg could indicate that sphalerite, at least, in the primary ore was rich in Hg. This is relatively common in massive, volcanic sulfide ore deposits, where Hg coexisting with different sulfides is preferentially hosted first by sphalerite, then by chalcopyrite and then by pyrite. The occurrence of Hg-rich sphalerite has been described in this type of ore deposit in British Columbia, Canada (Grammatikopoulos et al. 2006). The occurrence of secondary minerals comprising hydrated iron sulfates, gypsum and Fe–Mn oxides or oxyhydroxides typically reflects extensive weathering of primary minerals

in the tailings, where sulfate can form insoluble complexes with metals such as Ag, Pb, Sb, As, and Au. In fact, all of these elements except Au showed their maximum concentrations in this weathering zone. On the other hand, Pb concentrations were at a maximum from 10 to 40 cm depth, steadily decreasing from there downwards. This depth interval corresponded to a zone of abundant jarosite (10%, see Table 1), where Pb released from the weathering of galena was incorporated and immobilized in the form of plumbojarosite.

4.2.2 La Naya Mine Pond

The geochemical composition of the La Naya mine sludge was also characterized by high contents of heavy and transitional metals, but they were at least one order of magnitude lower than the Monte Romero values (Table 2, Fig. 4). The contents of Fe$_2$O$_{3\ total}$

Table 4 Correlation matrix between elements of the deep level (80 to 200 cm depth) of Monte Romero mine tailings (n=8; significance p<0,05)

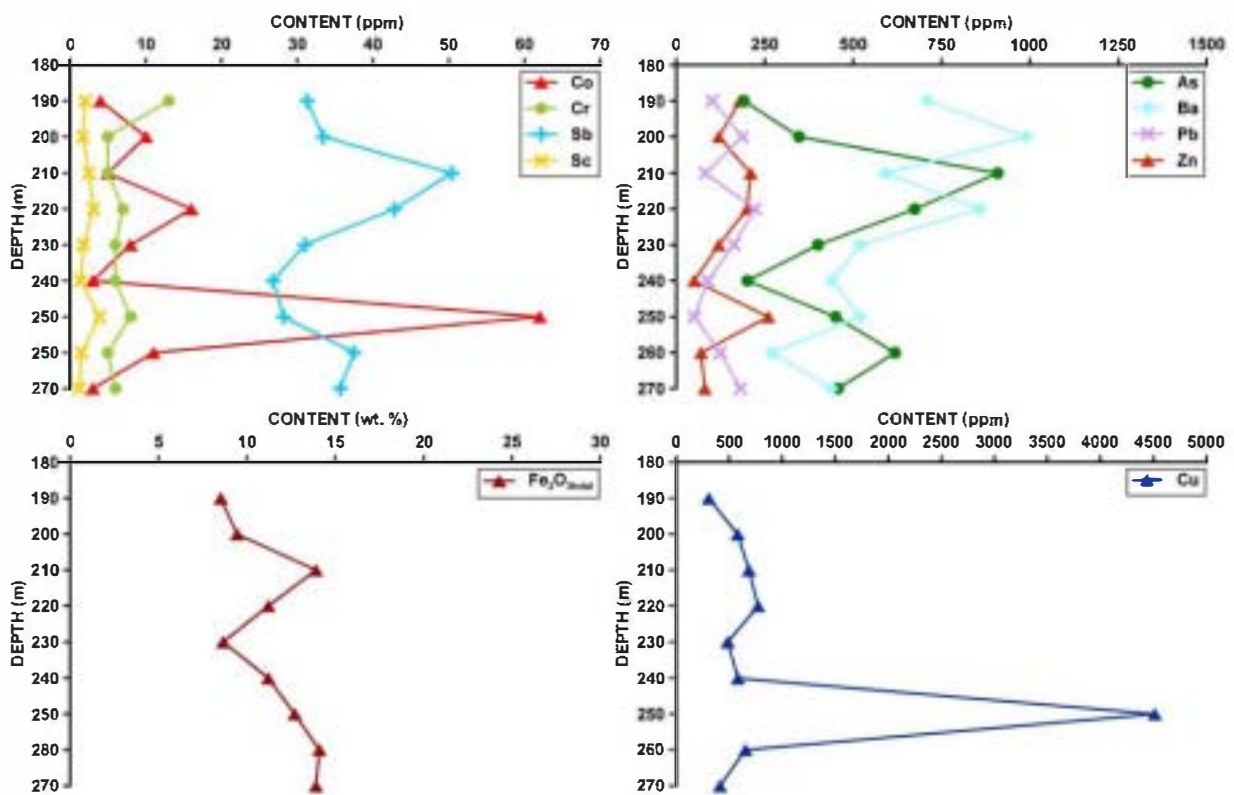|	Ag	As	Au	Ba	Co	Cu	Fe$_2$O$_{3\ tot}$	Hg	Pb	Sb	Zn
Ag	1.00										
As	0.09	1.00									
Au	0.66	0.48	1.00								
Ba	−0.35	0.28	−0.09	1.00							
Co	0.32	−0.04	0.15	−0.65	1.00						
Cu	0.87	0.00	0.52	−0.52	0.18	1.00					
Fe$_2$O$_{3\ tot}$	0.10	0.10	0.26	−0.64	0.90	0.04	1.00				
Hg	0.61	0.07	0.48	−0.19	−0.41	0.75	−0.42	1.00			
Pb	0.75	−0.01	0.17	−0.56	0.67	0.68	0.37	0.15	1.00		
Sb	0.97	0.04	0.71	−0.40	0.42	0.85	0.23	0.51	0.71	1.00	
Zn	0.58	−0.04	0.45	−0.21	−0.42	0.73	−0.43	0.99	0.10	0.49	1.00

Fig. 4 Distribution-with-depth profiles for total ferric iron and trace elements concentrations from La Naya mine tailings

and Sc were similar to the Monte Romero mine pond values, ranging between 8.5 and 14.1 wt.% and <4 ppm, respectively. The absence of elements such as Ag, Hg and Ni, and the absence of variations in the contents with depth, are significant features of these tailings (Lillo et al. 2008), contrasting with the geochemical features of the Monte Romero mine ponds. Arsenic, Sb and Fe_2O_3 total contents displayed a slight increase with depth whereas Au and Ba showed an inverse pattern (Fig. 4). Sample N-250 showed the highest Cu, Co, Sc and Zn contents and the lowest Au, Pb, and Sb contents. The contents of Ni were below the detection limit (20 ppm) in all of the analyzed samples.

At the La Naya mine pond, the concentrations of all of the elements were not only much lower, but also they showed practically no correlations between them (Table 5). Among the correlations that were present, the only prominent ones were those due to a high geochemical affinity, such as the positive As Sb correlation. This indicates that the original geochemistry in this pond has been almost completely transformed by the metallurgic processes of the ore minerals dumped in

the tailings. As in the superficial level of the Monte Romero mine ponds, Pb in La Naya showed almost no correlation with any of the other analyzed elements, which could be interpreted as resulting from the mining of galena.

4.3 Geometry of the Mine Pond Vessel

The internal and vessel geometries of the Monte Romero and La Naya mine ponds were determined from the electrical resistivity tomography survey.

4.3.1 Monte Romero Mine Ponds

The ERT profiles for the westernmost Monte Romero pond, where the tailings sampling was performed, are shown in Fig. 5. Profile 1 (longitudinal to the dyke) has a length of 141 m, with an electrode spacing of 3 m. The minimum absolute error during the inversion process was 7.8%, reached during the seventh iteration. The maximum penetration depth obtained was 13.5 m, and two units with very different resistivity values were identified (Fig. 5a).

Table 5 Correlation matrix between elements of the La Naya mine tailings ($n=9$; significance $p<0.05$)

	As	Au	Ba	Co	Cu	Fe$_2$O$_{3 \, tot}$	Pb	Sb	Zn
As	1.00								
Au	0.27	1.00							
Ba	−0.06	0.28	1.00						
Co	0.05	−0.38	−0.03	1.00					
Cu	0.04	−0.45	−0.11	0.98	1.00				
Fe$_2$O$_{3 \, tot}$	0.64	−0.47	−0.56	0.18	0.24	1.00			
Pb	0.07	0.28	0.46	−0.40	−0.52	−0.23	1.00		
Sb	0.91	0.40	0.16	−0.27	−0.29	0.46	0.22	1.00	
Zn	0.36	0.20	0.39	0.64	0.62	−0.02	−0.28	0.28	1.00

The upper unit A extended from 12 to 135 m along the profile, with lateral boundaries dipping steeply at the surface and flattening towards increasing depths, and exhibited the lowest resistivity values ranging from <1 to 25 ohm m. The lower unit B showed resistivity values ranging from 25 to >2,000 ohm m. The slightly undulating boundary between the two units was located, on average, at a depth of 3 m.

The length of the transverse profile 2 was 70.5 m, with an electrode spacing of 1.5 m and a maximum penetration depth of 7 m (Fig. 5b). The absolute error obtained during the inversion process was 2.3%, reached during the sixth iteration. In this profile, the thickness of unit A decreased from 3.5 m near the dam to 1.5 m far away from it. Furthermore, unit B was not as homogeneous as in profile 1, in such a way that two sectors with different resistivity values could be distinguished, which probably indicated differences in the degree of weathering of the shales: >88 ohm m southwards, and 25–88 ohm m from 25 m towards the north.

4.3.2 La Naya Mine Pond

Due to its greater dimensions in comparison to the Monte Romero mine ponds, the La Naya mine pond was surveyed in a single ERT profile, transverse to the dam (Fig. 6). This profile had a length of 235 m with an electrode spacing of 5 m, and reached a maximum penetration depth of 25 m. The minimum absolute error during the inversion process was 8.9%, reached during the sixth iteration. As in the Monte Romero mine ponds, two units with very different resistivity values were observed (Fig. 6b): an upper unit (unit A) located along the whole profile with resistivity values ranging from <1 to 30 ohm m; and a lower unit (unit B), with resistivity values ranging from 30 to 650 ohm m. However, in contrast to the Monte Romero mine ponds, unit A from La Naya was not homogeneous and two different subunits were identified: the first one (A1) extended from the beginning of the profile up to 185 m and was defined by resistivity values ranging from 10 to 70 ohm m. This subunit showed a maximum thickness of 10 m, decreasing towards the north. Below it, subunit A2 extended laterally from 185 m to the end of the profile and vertically down to 20 m depth. Subunit A2 exhibited a gradual change in resistivity values from 20 ohm m at the southern end to <1 ohm m towards the north. It is noteworthy that the lowest resistivity values were found along the 185–235 m interval of the profile. During the field survey, secondary sulfate patches were observed on the surface of the pond at this section of the profile. This is important since the relationship between the sulfate patches and the low resistivity values, indicating patches corresponding to surface areas with high water contents, define the recharge area of the pond. During the summer, when evaporation rates are at a maximum, evapotranspiration promotes oversaturation and the precipitation of sulfates in recharge areas. Unit A did not have a constant thickness: the maximum value (20 m) corresponded to the first 135 m of the profile, whereas at a distance of 150 m a sharp step existed in the base of the pond which decreased the thickness of unit A from 20 to 15 m.

4.4 Acid Water Flows

The low resistivity values associated with the occurrence of AMD allowed us to identify the presence of such acid waters and related subsurface flows in both the Monte Romero and La Naya mine ponds.
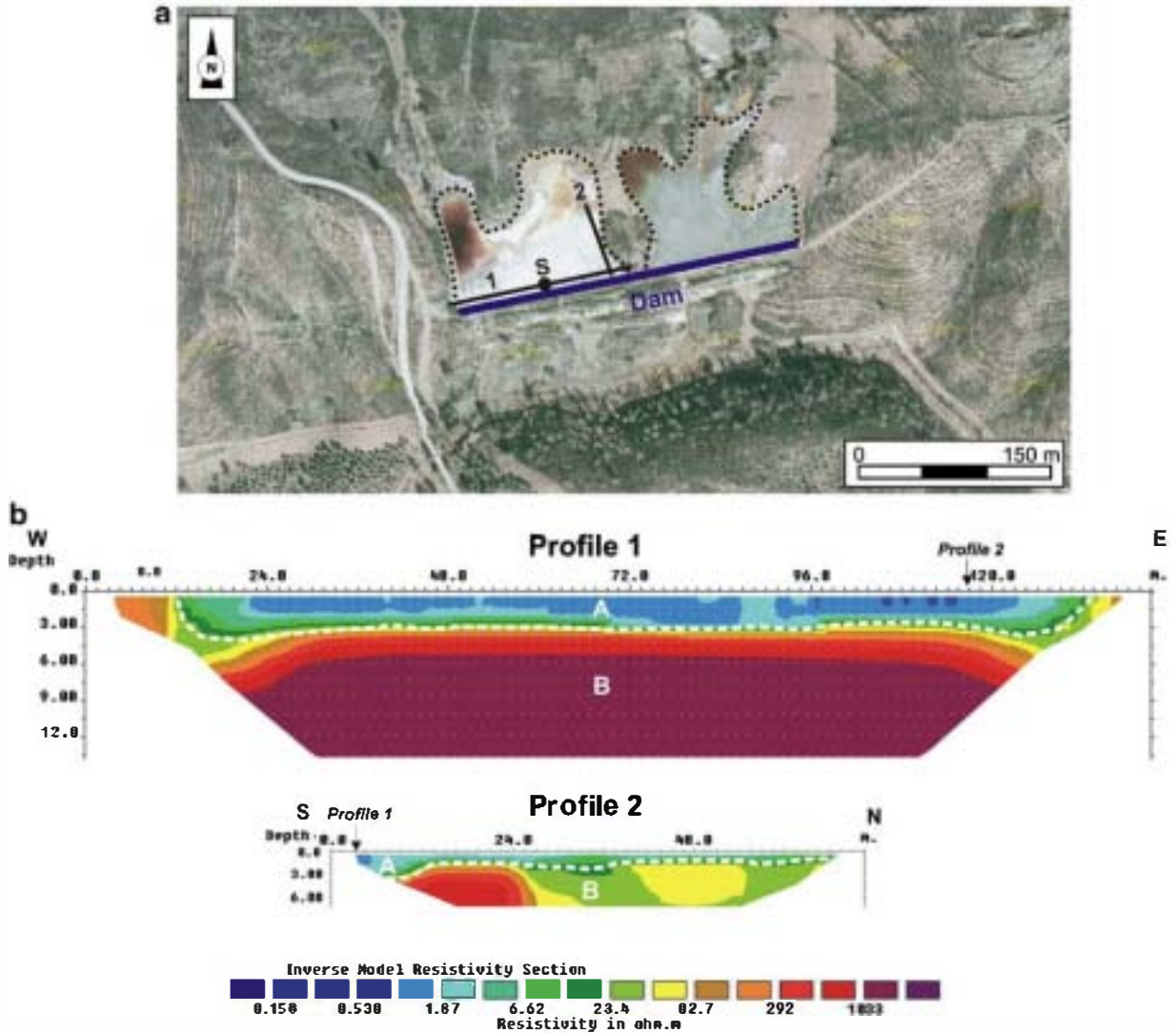
Fig. 5 a Location of ERT profiles (*lines 1–2*) and the tailings sampling (*s*) in the Monte Romero mine pond (*dotted line*); b Longitudinal (*1*) and transverse (*2*) ERT profiles. *White dashed lines* indicate the boundary between the tailings impoundment (unit *A*) and the Carboniferous shales (unit *B*)

The survey carried out at the Monte Romero mine pond showed that most of its unit A, interpreted as the pond infilling, showed resistivity values lower than 2 ohm m (Fig. 5b). These low values corresponded to water-saturated silt and clay materials with an abundance of sulfides, mainly pyrite. Moreover, the existence of a small trench in the western pond allowed us to identify the presence of the acid water table at a depth of 0.5 m (Fig. 2b). In addition to this, unit B, interpreted as being related to the Carboniferous shales which constitute

the base of the mine pond, exhibited very high and homogeneous resistivity values. This fact corroborates the theory that no acid water drainage occurred across the bedrock of the pond.

In contrast, the infilling of the La Naya mine pond had a more heterogeneous character. Its upper unit (unit A) could be divided into two different subunits (A1 and A2) according to their resistivity ranges (Fig. 6b). Subunit A2 exhibited the lowest resistivity values (<5 ohm m), extending from 65 m to the end of the profile. This was interpreted in terms of the
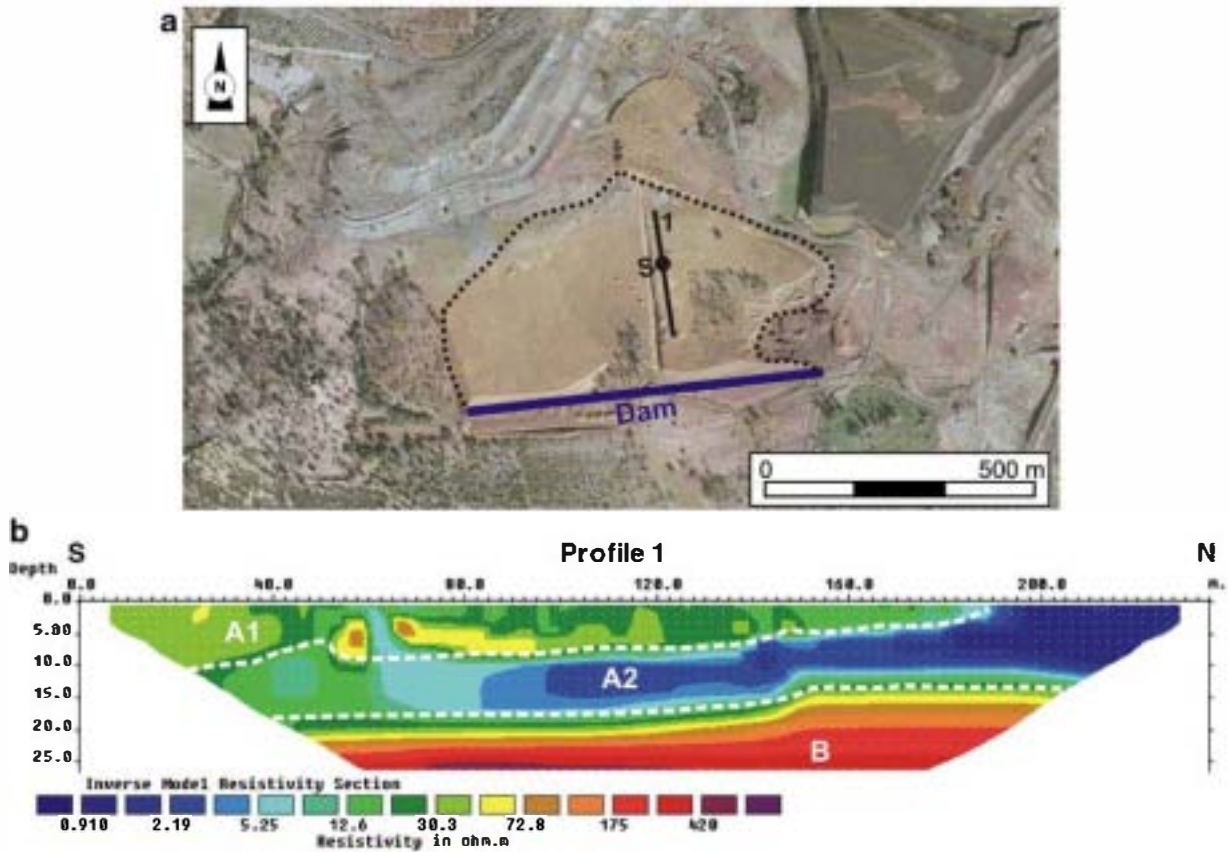
Fig. 6 a Location of the transverse ERT profile (*line 1*) and the tailings sampling (*s*) in the La Naya mine pond (*dotted line*); b ERT profile where are distinguished the tailings impoundment (*units A1–A2*) and the metamorphic-volcanic materials at the base (*unit B*)

occurrence of an inner groundwater flow which recharged the pond at its northeasternmost end, moved deeper into the pond towards the south, and finally emerged at the surface (at 65 m from the origin of the profile) due to the occurrence of a vertical low-permeability barrier. This barrier corresponded to an abandoned evacuation chimney constructed inside the mine pond that could be easily recognized on the surface. This interpretation agrees well with the occurrence of a small swamped zone in the field, located just on the low resistivity area (at 65 m from the origin of the profile). Unit B was much more homogeneous and corresponded to the metamorphic and volcanic rocks which constitute the base of the mine pond. Its high resistivity values, as was the case for the Monte Romero ponds, were also interpreted as being indicative of an absence of leakage through the bedrock; therefore, the internal groundwater flow described from the interpretation of unit A was confined to the interior of the pond.

4.5 Environmental Concerns

After the closure of the mining industry in the Huelva province during the last century, economic activities are now centered on agriculture, and the degradation of soil and water resources as a consequence of the oxidation of pyritic wastes has became a matter of concern. Specifically, agricultural soils in the surroundings of the two studied mine ponds (Cueva de la Mora and Riotinto ore deposits) are contaminated by Cu, Pb, Zn, and As. The contents of these contaminants exceed the 90th percentile of the geological dominium of the South Portuguese Zone (López et al. 2008). These features indicate that the cause of their enrichment in the soils must be leachates, mining spills or wind-blown dust from the mining facilities. Worldwide, the Tinto and Odiel rivers are two of the hydrological resources most affected by AMD (Cánovas et al. 2007; Hudson-Edwards et al. 1999; Sánchez España et al. 2005; Sarmiento et al. 2009). On the basis of pH levels and metal concentrations,

the waters of the Tinto river are mainly classified as high-acid high-metal, and those of the Odiel river are acid high-metal (Cánovas et al. 2007).

The metal contents in the Monte Romero levels (upper and deeper) significantly exceeded the Andalusian regional government legal limits for As, Cu, Hg, Pb, and Zn (Fig. 7) in agricultural soils (Aguilar et al. 1999). In contrast, the contaminant contents in the La Naya samples only exceeded the legal limits for As and Cu. It is important to determine how these metals can still be found. If they are present in the primary phases (sulfides, gangue, and host rock minerals) they represent a potential hazard when these minerals become affected by AMD processes. If the metals are incorporated in the secondary phases, it is important to evaluate the ability of these minerals to stably store these elements. The mineralogical characterization and the positive correlations confirmed that the metals are mostly present within sulfides in the deeper level of the Monte Romero ponds and that they can be released during weathering of the material containing them. The low metal content and the negative correlations reflect the nature of the dumped material in La Naya (poorly mineralized sludge and volcanic-bearing waste rocks), with a lower potential for the metals to be released.

Several papers have dealt with leachates from the wastes of the abandoned Cueva de la Mora and Monte Romero mines (Acero et al. 2007; Sánchez España et al. 2005). Weathering of the Monte Romero pyritic tailings generates acidic waters with high concentrations of potentially toxic contaminants (mainly Fe, Zn, Cu, Al, Mg and Ca). The pore-water pH measured by Acero et al. (2007) in the vadose zone remained

between 2.3 and 2.9, values which are similar to those determined in this study (Table 1). On the other hand, different remediation experiments on the Monte Romero wastes have focused on acid neutralization and metal retention in the sulfide tailings and the polluted streams by means of the addition of strongly alkaline substances (Caraballo et al. 2009; Pérez-López et al. 2007). However, there are no estimations of the total amounts of contaminant elements in the impoundment. In some mining deposits of the Iberian Pyrite Belt, the contribution of toxic elements has been determined as the basis for the assessment of their environmental impacts in case of a dam collapse or rainfall erosion (Álvarez-Valero et al. 2008, 2009; Pérez-López et al. 2008). In this particular case, the maximum amounts of potential contaminants were obtained taking into account the mean content of potentially toxic elements (Table 1, As, Co, Cu, Hg, Pb, Sb, and Zn) and the volume and mass of the wastes (Table 6). The volume of tailings was calculated including the mean depth from the electrical resistivity profiles and assuming wedge geometry (Fig. 5). The easternmost mine pond, with a trough geometry (Gómez-Ortiz et al. 2010), was also included in the estimation because of the identical mining histories of both ponds. Even though geophysical analysis showed two different units in each impoundment, a mean bulk density of 2.64 g/cm^3 was calculated from the mineral particle density and the porosity (%) given by Acero et al. (2007) for these tailings. These authors calculated a bulk density of 2.24 g/cm^3 for the first 70 cm. The significant content of denser minerals (pyrite, sphalerite, and barite) identified at the deeper level highly increased

Fig. 7 Composition of Monte Romero (*UL* upper level, *DL* deep level) and La Naya samples (selected hazardous minor and trace elements) normalized to the Andalusian law limits for concentrations in agricultural soils (from Aguilar et al. 1999)
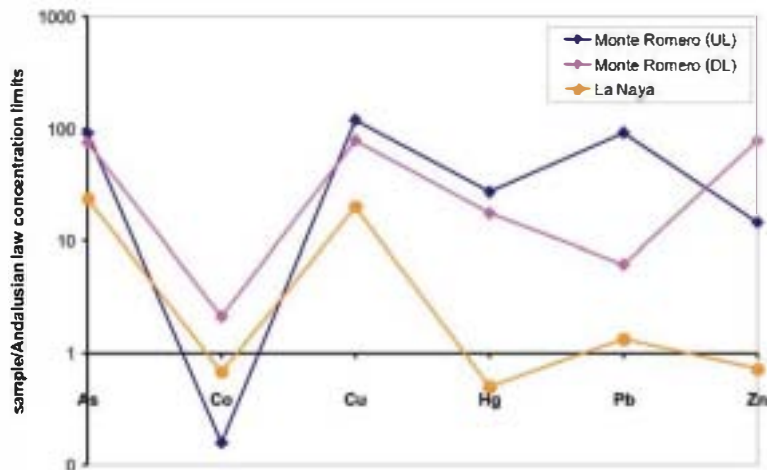
Table 6 Main physical features of the mine ponds and amounts of metals contained in the tailings

Mine pond	Area (m^2)	Average thickness (m)	Volume (m^3)	Mass (t)	Total element amount (t)							
					As	Co	Cu	Hg	Pb	Sb	Zn	Σ
Monte Romero W	8854	3	13281	35041	58	1	171	1	162	12	336	740
Monte Romero E	7549	3.5	26422	69710	115	2	340	2	322	24	669	1473
La Naya	100430	17.5	1757525	3277784	1548	44	3272	–	437	115	470	5887

the mean bulk density of the ponds. The metals presented in the Monte Romero sludge amount more than 2,200 t (Table 6). Despite the relatively small dimensions of this mine residue, an intense rainfall episode could release its toxic load along the Monte Romero creek and reach the Olivargas reservoir (4 km downstream), producing serious effects on water quality and aquatic life.

The oxide terraces in the Tinto River and the ferruginous paleosols that pre-date the Pliocene highlight a natural origin o the headwaters enriched in sulfuric acid and ferric iron (Fernández-Remolar et al. 2005). However, the extensive mine deposits of the Riotinto district, in the catchment area of the Tinto River, are an important source of AMD and have seriously altered the environment (Hudson-Edwards et al. 1999; Romero et al. 2006). Specifically, the pH value in the stretch near the La Naya mine pond is only 1.6. The potential toxicity of the metal content in this mining residue was also determined (Table 6). The bulk density was calculated from the mineral particle density assuming a porosity of 50%, and a mean value for mine the ponds was derived from the processing of these types of Ag–Au–Pb–Zn deposits (Bjelkevik and Knutsson 2005). Thus, the La Naya impoundment contains more than 5,800 t of potentially toxic elements. Despite the great volume occupied by this deposit, its potential impact is proportionately less than the Monte Romero sludge since the tailings of this deposit have been reworked and have lower concentrations of metals. However, although the upper unit does not contain pyrite or any other sulfides (Table 1), the dissolution of the sulfate phases (jarosite) could transfer their metal contents to the environment and contribute to potential global toxicity. Moreover, tailings erosion is significant in the southeastern sector of the waste.

The volume of the La Naya mine pond is similar to the sludge involved in the Aznalcóllar mining accident, whereas the Monte Romero deposit only represents a small fraction. The pyrite tailings which spilled from Aznalcóllar into the de Agrio and Guardiamar rivers contained very high levels of several metals: As (4,300–4,500 ppm), Cu (1,438–2,095 ppm), Hg (15.38–16.90 ppm), Pb (8,389–10,493 ppm), and Zn (5,546–7,880 ppm; Galán et al. 2002). Despite the different remediation actions which were carried out, there is still a residual pollution in the soils and sediments which exceeds the advisable limits for cultivation (Aguilar et al. 2004, 2007; Galán et al. 2002; Hudson-Edwards et al. 2003). The comparison of this geochemical composition with Table 2 highlights the lower metal contents of the La Naya impoundment. Metal contents of the Monte Romero mine ponds exceed the Aznalcóllar values. Therefore, in the case of a dam failure, the potential impact of the Monte Romero sludge would have a similar effect on water and soil quality due to its metal load, although a significantly smaller area would be affected.

Finally, the pollutant potential of the sulfide tailings depends on their capacity to release toxic elements (which can be evaluated by means of a sequential extraction procedure, e.g., Álvarez-Valero et al. 2009; Pérez-López et al. 2008), and the chemical species involved in the mobilization of metals. Therefore, future work in these mine ponds must be focused on the factors controlling the bio-availability of heavy metals.

5 Conclusions

The two selected deposits from the Iberian Pyrite Belt (Spain) display different mineralogies, physico-chemical parameters, chemical compositions of the tailings, and pond conditions. The Monte Romero mine tailings show an upper level mainly composed of silicate phases and a

deeper level mainly composed of sulfide and barite. In both levels, the potentially toxic metal content is different but high enough to exceed the regional legal concentration limits for agricultural soils. The electrical resistivity tomography survey revealed a homogeneous upper unit corresponding to water-saturated silt and clay materials with an abundance of sulfides, which was interpreted as the pond infilling. The La Naya mine pond presents a homogeneous mineralogical composition made up of quartz as main mineral and chlorite-smectite and jarosite as accessory phases. The absence of sulfide phases and the low contents of metal elements are directly related to the reworking processes of the sludge dumped in this pond. The geophysical survey revealed that the pond infilling range is between 15 and 20 m. An inner groundwater flow in the infilling was recognized. The low resistivity values allowed the presence of acid waters and related subsurface flows to be identified in both the Monte Romero and La Naya mine ponds, but no acid water drainage occurs across their vessels. When compared to the Aznalcóllar tailings spill, the La Naya pond is large enough to release a similar amount of sludge, but of a very low metal content. The Monte Romero sludge displays a similar toxic metal content to the Aznalcóllar sludge, but its size is significantly lower. This work revealed that the joint use of geophysical and geochemical techniques allows a complete environmental characterization of mine sludge structures, allowing the monitoring and estimations of potential pollution.

References

Acero, P., Ayora, C., & Carrera, J. (2007). Coupled thermal, hydraulic and geochemical evolution of pyritic tailings in unsaturated column experiments. *Geochimica et Cosmochimica Acta, 71*, 5325–5338.

Aguilar, J., Dorronsoro, C., Gómez Ariza, J.L., & Galán, E. (1999). *Los criterios y estándares para declarar un suelo contaminado en Andalucía y la metodología y técnica de toma de muestras y análisis para su investigación*. Andalucía: Consejería de Medio Ambiente de la Junta de Andalucía.

Aguilar, J., Dorronsoro, C., Fernández, E., Fernández, J., García, I., Martín, F., et al. (2004). Soil pollution by a pyrite mine spill in Spain: evolution in time. *Environmental Pollution, 132*, 395–401.

Aguilar, J., Dorronsoro, C., Fernández, E., Fernández, J., García, I., Martín, F., et al. (2007). Arsenic contamination in soils affected by a pyrite-mine spill (Aznalcóllar, SW Spain). *Water, Air, and Soil Pollution, 180*, 271–281.

Álvarez-Valero, A. M., Pérez-López, R., Matos, J., Capitán, M. A., Nieto, J. M., Sáez, R., et al. (2008). Potential environmental impact at São Domingos mining district (Iberian Pyrite Belt, SW Iberian Peninsula): evidence from a chemical and mineralogical characterization. *Environmental Geology, 55*, 1797–1809.

Álvarez-Valero, A. M., Sáez, R., Pérez-López, R., Delgado, J., & Nieto, J. M. (2009). Evaluation of heavy metal bio-availability from Almagrera pyrite-rich tailings dam (Iberian Pyrite Belt, SW Spain) based on a sequential extraction procedure. *Journal of Geochemical Exploration, 102*, 87–94.

Bernard, J. (2003). *Short note on the depth of investigation of electrical methods*. France: IRIS.

Bjelkevik, A., & Knutsson, S. (2005). Swedish tailings—comparison of mechanical properties between tailings and natural geological materials. In *Proceedings securing the future, International Conference on Mining and the Environment Metals and Energy Recovery* (pp. 117–129). Stockholm: Svemin.

Blanco, A., Lloret, A., Carrera, J., Saaltink, M. W., Acero, P., Ayora, C., et al. (2003). Monitorización del movimiento del agua a través de una balsa de lodos residuales mineros en la Faja Pirítica Ibérica (SO de la Península Ibérica). In *Jornadas Luso-Españolas sobre Aguas Subterráneas en el Sur de la Península Ibérica* (pp. 1–10). Portugal: Asociación Portuguesa de Recursos Hídricos.

Cánovas, C. R., Olías, M., Nieto, J. M., Sarmiento, A. M., & Cerón, J. C. (2007). Hydrogeochemical characteristics of the Odiel and Tinto rivers SW Spain. Factors controlling metal contents. *Science of the Total Environment, 373*, 363–382.

Cánovas, C. R., Hubbard, C. G., Olías, M., Nieto, J. M., Black, S., & Coleman, M. L. (2008). Hydrochemical variations and contaminant load in the Río Tinto Spain during flood events. *Journal of Hydrology, 350*, 25–40.

Caraballo, M., Rötting, T. S., Macías, F., Nieto, J. M., & Ayora, C. (2009). Field multi-step limestone and MgO passive system to treat acid mine drainage with high metal concentrations. *Applied Geochemistry, 24*, 2301–2311.

Chopin, E. I. B., & Alloway, B. J. (2007). Trace element partitioning and soil particle characterisation around mining and smelting areas at Tharsis, Ríotinto and Huelva, SW Spain. *The Science of the Total Environment, 373*, 488–500.

Fernández-Caliani, J. C., Barba-Brioso, C., & De la Rosa, J. D. (2009). Mobility and speciation of rare earth elements in acid minesoils and geochemical implications for river waters in the southwestern Iberian margin. *Geoderma, 149*, 393–401.

Fernández-Remolar, D. C., Morris, R. V., Gruener, J. E., Amils, R., & Knoll, A. H. (2005). The Río Tinto Basin, Spain: mineralogy, sedimentary geobiology, and implications for interpretation of outcrop rocks at Meridiani Planum, Mars. *Earth and Planetary Science Letters, 240*, 149–167.

Galán, E., González, I., & Fernández-Caliani, J. C. (2002). Residual pollution load of soils impacted by the Aznalcóllar (Spain) mining spill after clean-up operations. *The Science of the Total Environment, 286*, 167–179.

Gómez-Ortiz, D., Martín-Velázquez, S., Martín-Crespo, T., De Ignacio-San José, C., & Lillo-Ramos, J. (2010). Application of electrical resistivity tomography to the environmental characterization of abandoned massive sulphide mine ponds (Iberian Pyrite Belt, SW Spain). *Near Surface Geophysics, 8*, 65–74.

Grammatikopoulos, T. A., Valeyev, O., & Roth, T. (2006). Compositional variation in Hg-bearing sphalerite from the polymetallic Eskay Creek deposit, British Columbia, Canada. *Chemie der Erde - Geochemistry, 66*, 307–314.

Hudson-Edwards, K., Schell, C., & Macklin, M. G. (1999). Mineralogy and geochemistry of alluvium contaminated by metal mining in the Río Tinto area, southwest Spain. *Applied Geochemistry, 14*, 1015–1030.

Hudson-Edwards, K. A., Macklin, M. G., Jamieson, H. E., Brewer, P. A., Coulthard, T. J., Howard, A. J., et al. (2003). The impact of tailings dam spills and clean-up operations on sediment and water quality in river systems: the Ríos Agrio–Guadiamar, Aznalcóllar, Spain. *Applied Geochemistry, 18*, 221–239.

IGME. (1998). *Inventario nacional de balsas y escombreras. Unpublished database.* Madrid: IGME (Instituto Geológico y Minero de España).

Jambor, J. L., & Owens, D. R. (1993). *Mineralogy of tailings impoundment at the former Cu–Ni deposit of Nickel Rim Mines Ltd. Eastern edge of the Sudbury structure, Ontario. Division Report MSL 93-4 (CF), CANMET.* Canada: Energy, Mines and Resources.

Leistel, J. M., Marcoux, E., Thiéblemont, D., Quesada, C., Sánchez, A., Almodóvar, G. R., et al. (1998). The volcanic-hosted massive sulphide deposits of the Iberian Pyrite Belt. Review and preface to the Thematic Issue. *Mineralium Deposita, 33*, 2–30.

Lillo, F., Martín-Crespo, T., Gómez-Ortiz, D., de Ignacio, C., & Martín-Velázquez, S. (2008). Geochemical characterization of mining ponds of the Iberian Pyrite Belt. *Geotemas, 10*, 1401–1404.

Loke, M. H. (2004). (PDF). Tutorial: 2-D and 3-D electrical imaging surveys. www.geoelectrical.com.

Loke, M. H., & Barker, R. D. (1995). Least-square deconvolution of apparent resistivity pseudo-sections. *Geophysics, 60*, 499–523.

Loke, M. H., & Barker, R. D. (1996). Rapid least-squares inversion of apparent resistivity pseudosections by a quasi-Newton method. *Geophysical Prospecting, 44*, 131–152.

López, M., González, I., & Romero, A. (2008). Trace elements contamination of agricultural soils affected by sulphide exploitation (Iberian Pyrite Belt, SW Spain). *Environmental Geology, 54*, 805–818.

Martín-Crespo, T., de Ignacio-San José, C., Gómez-Ortiz, D., Martín-Velázquez, S., & Lillo, J. (2010). Monitoring study of the mine pond reclamation of Mina Concepción, Iberian Pyrite Belt (Spain). *Environmental Earth Sciences, 54*, 1275–1284.

Martínez-Pagán, P., Faz-Cano, A., Aracil, E., & Arocena, J. M. (2009). Electrical resistivity tomography revealed the spatial chemical properties of mine tailings ponds in the Sierra Minera (SE Spain). *Journal of Environmental and Engineering Geophysics, 14*, 63–76.

Nocete, F., Alex, E., Nieto, J. M., Saéz, R., & Bayona, M. R. (2005). An archaeological approach to regional environmental pollution in the South-western Iberian Peninsula related to Third Millenium B.C mining and metallurgy. *Journal of Archaeological Science, 32*, 1566–1576.

Pérez-López, R., Cama, J., Nieto, J. M., & Ayora, C. (2007). The iron-coating role on the oxidation kinetics of a pyritic sludge doped with fly ash. *Geochimica et Cosmochimica Acta, 71*, 1921–1934.

Pérez-López, R., Álvarez-Valero, A. M., Nieto, J. M., Sáez, R., & Matos, J. X. (2008). Use of sequential extraction procedure for assessing the environmental impact at regional scale of the São Domingos Mine (Iberian Pyrite Belt). *Applied Geochemistry, 23*, 3452–3463.

Reynolds, J. M. (1997). *An introduction to applied and environmental geophysics.* Chichester: Wiley.

Romero, A., González, I., & Galán, E. (2006). Estimation of potential pollution of waste mining dumps at Peña del Hierro (Pyrite Belt, SW Spain) as a base for future mitigation actions. *Applied Geochemistry, 21*, 1093–1108.

Ruiz, F., Gonzalez-Regalado, M. L., Borrego, J., Morales, J. A., Pendón, J. G., & Muñoz, J. M. (1998). Stratigraphic sequence, elemental concentrations and heavy metal pollution in Holocene sediments from the Tinto-Odiel Estuary, Southwestern Spain. *Environmental Geology, 34*, 270–278.

Sáez, R., Almodóvar, G. R., & Pascual, E. (1996). Geological constraints on massive sulphide genesis in the Iberian Pyrite Belt. *Ore Geology Reviews, 11*, 429-451.

Sánchez España, J., López, P. E., Santofimia, P. E., Aduvire, O., Reyes, J., & Barettino, D. (2005). Acid mine drainage in the Iberian Pyrite Belt (Odiel river watershed, Huelva, SW Spain): geochemistry, mineralogy and environmental implications. *Applied Geochemistry, 20*, 1320–1356.

Sánchez España, E. J., López, P. E., Santofimia, E., & Díez Ercilla, M. (2008). The acidic mine pit lakes of the Iberian Pyrite Belt: an approach to their physical limnology and hydrogeochemistry. *Applied Geochemistry, 23*, 1260–1287.

Sarmiento, A. M., Nieto, J. M., Olías, M., & Cánovas, C. R. (2009). Hydrochemical characteristics and seasonal influence on the pollution by acid mine drainage in the Odiel river Basin (SW Spain). *Applied Geochemistry, 24*, 697–714.

Sasaki, Y. (1992). Resolution of resistivity tomography inferred from numerical simulation. *Geophysical Prospecting, 40*, 453-464.

Siegel, F. R. (2002). *Environmental geochemistry of potentially toxic metals.* Berlin: Springer.

Telford, W. M., Geldart, L. P., Sheriff, R. E., & Keys, D. A. (1990). *Applied geophysics.* Cambridge: Cambridge University Press.

Tornos, F. (2006). Environment of formation and styles of volcanogenic massive sulfides: the Iberian Pyrite Belt. *Ore Geology Reviews, 28*, 259–307.

US EPA. (1993). *Clean Water Act. Section 503. Vol. 58, No. 32.* Washington: U.S. Environmental Protection Agency.

van Geen, A., Adkins, J. F., Boyle, E. A., & Palanques, A. (1997). A 120 year record of widespread contamination from mining of the Iberian Pyrite Belt. *Geology, 25*, 291–294.

Vick, S. G. (1990). *Planning, design and analysis of tailings dams.* Vancouver: BiTech.